

# The Blake geomagnetic excursion recorded in a radiometrically dated speleothem

María-Luisa Osete<sup>a,b,\*</sup>, Javier Martín-Chivelet<sup>b,c</sup>, Carlos Rossi<sup>d</sup>, R. Lawrence Edwards<sup>e</sup>, Ramon Egli<sup>f</sup>, M. Belén Muñoz-García<sup>c</sup>, Xianfeng Wang<sup>g</sup>, F. Javier Pavón-Carrasco<sup>a</sup>, Friedrich Heller<sup>h</sup>

<sup>a</sup> Dept. Física de

<sup>b</sup> Instituto de Geociencias (IGEO) CSIC-UCM, Ciudad Universitaria, 28040 Madrid, Spain

<sup>c</sup> Dept. Estratigrafía, Facultad de Ciencias Geológicas, Universidad Complutense, 28040 Madrid, Spain

<sup>d</sup> Dept. Petrología y Geoquímica, Facultad de Ciencias Geológicas, Universidad Complutense, 28040 Madrid, Spain

<sup>e</sup> Department of Geology and Geophysics, University of Minnesota, MN 55455, USA

<sup>f</sup> Department für Geo- und Umweltwissenschaften, Ludwig-Maximilians Universität, 80333 München, Germany

<sup>g</sup> Earth Observatory of Singapore, Nanyang Technological University, Singapore 639798, Singapore

<sup>h</sup> Institut für Geophysik, ETH-Zentrum, CH-8092 Zürich, Switzerland

la Tierra I, Facultad de Ciencias Físicas,

## A B S T R A C T

One of the most important developments in geomagnetism has been the recognition of polarity excursions of the Earth's magnetic field. Accurate timing of the excursions is a key point for understanding the geodynamo process and for magnetostratigraphic correlation. One of the best-known excursions is the Blake geomagnetic episode, which occurred during marine isotope stage MIS 5, but its morphology and age remain controversial. Here we show, for the first time, the Blake excursion recorded in a stalagmite which was dated using the uranium-series disequilibrium techniques. The characteristic remanent magnetisation is carried by fine-grained magnetite. The event is documented by two reversed intervals (B1 and B2). The age of the event is estimated to be between 116.5 ± 0.7 kyr BP and 112.0 ± 1.9 kyr BP, slightly younger (~3–4 kyr) than recent estimations from sedimentary records dated by astronomical tuning. Low values of relative palaeointensity during the Blake episode are estimated, but a relative maximum in the palaeofield intensity coeval with the complete reversal during the B2 interval was observed. Duration of the Blake geomagnetic excursion is 4.5 kyr, two times lower than single excursions and slightly higher than the estimated diffusion time for the inner core (~3 kyr).

### Keywords:

geomagnetic excursions  
speleothems  
radioisotope geochronology  
palaeointensity  
rock magnetism  
quaternary geochronology

## 1. Introduction

Understanding the origin, duration and the field behaviour associated with excursions is a forefront research area within solid earth geophysics (Roberts, 2008). Precise evaluation of the duration of geomagnetic excursions has become a point of interest since Gubbins (1999) proposed that excursions occurred when the field in the Earth's liquid core reverses polarity without accompanying field reversal in the solid inner core.

This mechanism and the corresponding estimation of diffusion times for the inner core provide a prediction for excursion duration: around 3 kyr. This model has become a standard explanation for excursions. However, precise duration of some excursions is still unknown.

The Blake geomagnetic excursion was first identified by Smith and Forster (1969). Since then it has been reported in different records, including oceanic sediments (Tric et al., 1991; Thouveny et al., 2004; Lund et al., 2006) lacustrine sediments (Creer et al., 1980), loess deposits (Zhu et al., 1994; Reinders and Hambach, 1995; Fang et al., 1997) and continental sediments (Shier et al., 2011). But the morphology and age of the event still remain controversial. It seems to be characterised by two reversed polarity zones (Denham, 1976) or even by a single polarity zone (Tucholka et al., 1987). Age and duration estimates vary significantly in the literature. Extreme discrepancies for the onset of the Blake event have been given with 138 kyr BP and 100 kyr (Bleil and Gard (1989), and Denham (1976), respectively). Duration estimates range between 20 and 35 kyr (Denham, 1976) with a

\* Corresponding author at: Dept. Física de la Tierra I, Facultad de Ciencias Físicas, Universidad Complutense, 28040 Madrid, Spain. Tel: +34913944396; fax: +34913944398.

E-mail addresses: mlosete@fis.ucm.es (M. -L. Osete), j.m.chivelet@geo.ucm.es (J. Martín-Chivelet), crossi@geo.ucm.es (C. Rossi), edwar001@umn.edu (R. Lawrence Edwards), egli@geophysik.uni-muenchen.de (R. Egli), mbmunoz@geo.ucm.es (M. Belé. Muñoz-García), xianfeng.wang@ntu.edu.sg (X. Wang), fj.pavon@fis.ucm.es (F. Javier Pavón-Carrasco), heller@mag.ig.erdw.ethz.ch (F. Heller).

minimum value of around 5 kyr introduced by Tucholka et al. (1987). Studies on marine sediments suggest that this excursion occurred during marine isotope stage MIS 5, probably during substages 5e/5d (Thouveny et al., 2004; Channell, 2006). The general consensus is that the Blake event took place between 125 and 110 kyr (Lund et al., 2006; Thouveny et al., 2004; Langereis et al., 1997), but absolute dating of the event is still lacking.

Calcite speleothems, such as stalagmites and flowstones, have an enormous potential in palaeomagnetism, since they may grow continuously through thousands of years, thereby preserving the palaeomagnetic signal at the time of calcite precipitation (Latham et al., 1979a, 1979b, 1987; Openshaw et al., 1993). The lock-in of the magnetisation is nearly instantaneous, and post-depositional effects are usually not very significant (Lascu and Feinberg, 2011). In addition, ages of speleothems can be determined with the high precision U-series radiometric dating techniques (e.g., Dorale et al., 2004).

Despite the great potential of speleothems for palaeomagnetic studies, the typically very low concentration of ferromagnetic minerals resulting in low Natural Remanent Magnetisation (Perkins and Maher, 1993; Perkins, 1996) has limited their usage. To our knowledge, no excursions have been unambiguously reported from a speleothem. In this paper, we provide for the first time radiometric and palaeomagnetic evidence for the age and characteristics of the Blake event that has been recorded in a speleothem in northern Spain.

## 2. Studied material: C8 Stalagmite

Stalagmite C8 was collected from Cobre Cave in northern Spain (42°59'N, 4°22'W, elevation ~1600 m). This cave is located in the Sierra de Peñalabra, on the southern watershed of the Cantabrian Mountains (Fig. 1A). The cave has been developed in Carboniferous limestones and consists of an active low-gradient stream passage at the water table, and several relict low-gradient canyons at higher elevations (Rossi et al., 1997). The studied stalagmite was retrieved from a relict canyon, ~1200 m distant from the cave entrance, 63 m above the resurgence elevation, and ~100 m below the ground surface. The C8 sampling site is quite isolated from anthropogenic disturbance and external short-term

environmental changes, with an air temperature of  $5.5 \pm 0.3$  °C and a relative humidity of  $98\% \pm 2\%$ .

The recovered portion of C8 is 68 cm long, 15 cm wide at the base, and shows a roughly conical shape (Fig. 1B). Axial cross-sections of C8 reveal an internal structure formed by light-brown to white, millimetric to centimetric-scale alternating bands, with no obvious indications of significant growth hiatuses (Fig. 1C and D). Both types of layers further contain internal growth laminae of micrometric scale (10–100 μm thick), more apparent in the flanks of the sample, and defined by variations in the abundance of aqueous fluid inclusions.

Previous work on stalagmite C8 includes petrographic and stable isotope analyses (Muñoz-García, 2007; Muñoz-García et al., 2007). As a whole, C8 shows no obvious signs of alteration or recrystallisation. Transmitted-light petrographic study using ~500 μm-thick polished sections revealed that C8 is formed by highly transparent and relatively large calcite crystals (mm–cm), elongated in the direction of growth and with length/width ratios usually between 6 and 10 (columnar fabric according to Frisia et al. (2000)). This is a typical primary fabric that precipitates by slow degassing of CO<sub>2</sub> at or very close to conditions of isotopic equilibrium (Frisia et al., 2000). The stable isotope record of C8 includes a series of δ<sup>18</sup>O analyses performed along the growth axis (Fig. 2b). δ<sup>18</sup>O values range between –7.08‰ and –8.69‰ (VPDB), and vertical changes in these values outline four successive stratigraphic intervals, each of them defined by a consistent trend. These δ<sup>18</sup>O changes mainly reflect variations in the isotopic composition of seepage water, which are in turn largely controlled by the average composition of local meteoric waters (Muñoz-García, 2007). Cold intervals (as cold stadials) are positively correlated with lower values in the δ<sup>18</sup>O, whereas warmer ones (as interstadials) show higher values. The isotopic record of C8 will be herein used as a reference to compare our palaeomagnetic results with previous sedimentary records of the Blake excursion the ages of which were constrained by astronomical tuning of the marine isotope stages.

## 3. Methods

Prior to its removal from the cave, C8 was oriented *in situ* using a magnetic compass and an inclinometer. 31 cubic

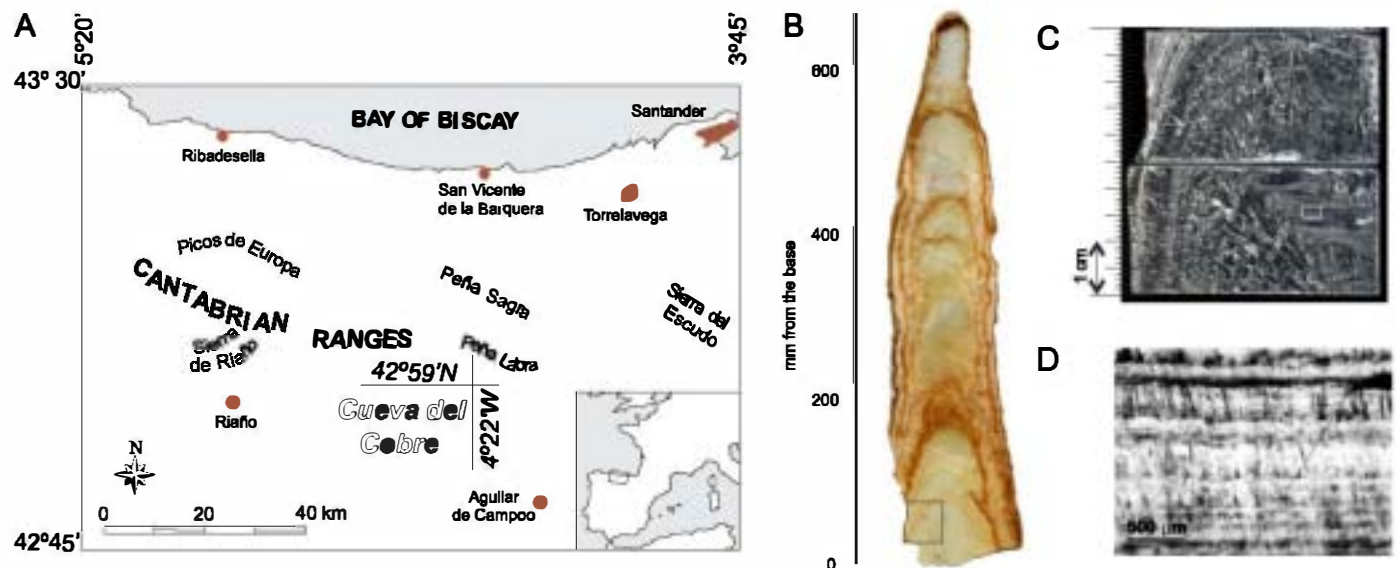
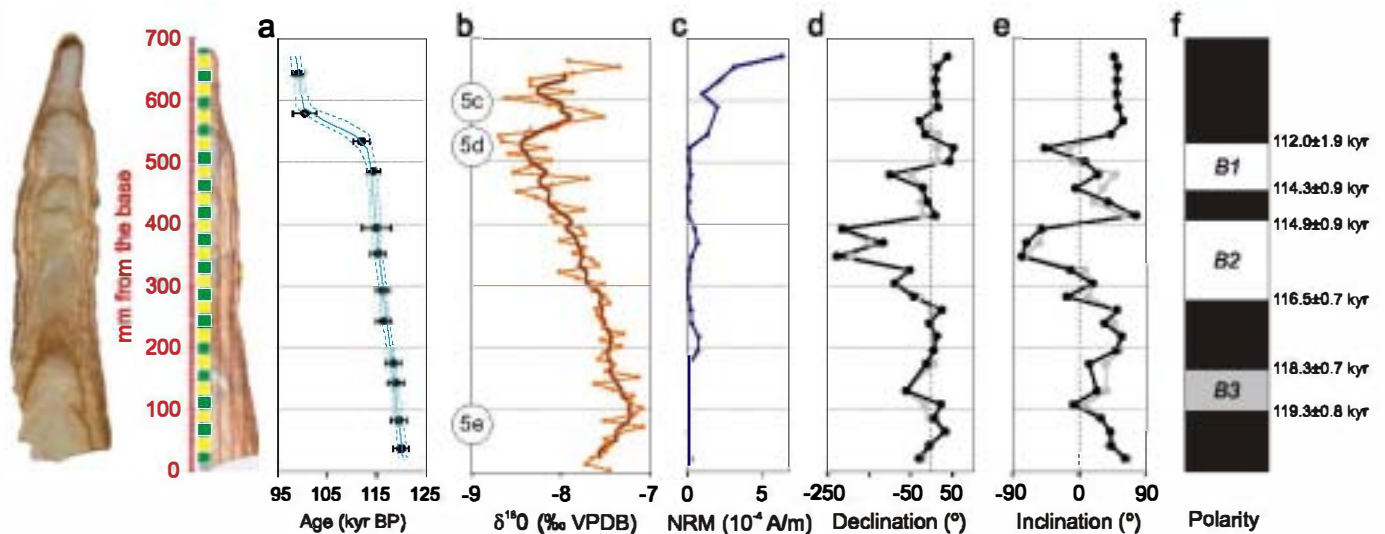


Fig. 1. Location and details of the C8 stalagmite. (A) Location maps of the studied stalagmite, (B) longitudinal section of stalagmite C8, (C) transmitted light view of two sections (approximately 500 μm thick) of the axial part of C8 shown in figure B. Regular growth laminae can be observed. (D) Detail from marked rectangle in figure C under petrographic microscopy.



**Fig. 2.** Palaeomagnetic, chronostratigraphic and isotopic results. Left: studied stalagmite and location of palaeomagnetic samples (cubes); (a) U–Th dates and age model; (b)  $\delta^{18}O$  record; (c) initial NRM intensity; (d, e) ChRM declination and inclination values and comparison with the NRM values (in grey); (f) magnetostratigraphic column with normal (black), reversed (white) and ambiguous (grey) zones.

samples ( $8 \text{ cm}^3$ ) were cut from the central part of an axial section of the stalagmite and used for palaeomagnetic analysis (Fig. 2, left). Palaeomagnetic studies were carried out at the Institut für Geophysik, ETH Zürich, Switzerland. The natural remanent magnetisation (NRM) of the samples was measured using a three-axis 2G-Enterprise cryogenic magnetometer. Samples were subjected to both thermal (TH) and alternating field (AF) demagnetisation cleaning. Stepwise TH demagnetisation of NRM was carried out in 20–50 °C steps up to 580–700 °C. Six samples exploded during heating at 300–650 °C, most likely due to the decrepitating of the abundant aqueous fluid inclusions. Stepwise AF demagnetisation was conducted in 2–20 mT steps up to 140 mT. 17 samples were subjected to AF demagnetisation. After demagnetisation of these samples, an anhysteretic remanent magnetisation (ARM) was imparted at 200 mT followed by very detailed AF demagnetisation and finally acquisition of isothermal remanent magnetisation (IRM) at 200 mT. These experiments were conducted to study the magnetic properties variations (Supplementary Table S1) and to perform relative palaeointensity (RPI) analyses (Tauxe, 1993). Stepwise acquisition of isothermal remanent magnetisation (IRM) up to 1800 mT followed by isothermal remagnetisation in three orthogonal directions and subsequent progressive thermal demagnetisation were carried out on selected samples in order to identify the magnetic mineralogy of the samples (Lowrie, 1990). The field applied along the three orthogonal axes was 1800 mT, 400 mT and 250 mT.

Thirteen  $\sim 200$  mg sub-samples were retrieved from C8 along selected growth layers and prepared for  $^{230}\text{Th}$  dating following procedures similar to those described by Edwards et al. (1987) and Dorale et al. (2004). Analyses were conducted in the Minnesota Isotope Laboratory of the University of Minnesota by means of an inductively coupled plasma mass spectrometer (ThermoFinnigan ELEMENT) using procedures described in Shen et al. (2002) and Dorale et al. (2004).

#### 4. Age model

The age model for stalagmite C8 was based on thirteen  $^{230}\text{Th}$  dates (summarised in Table 1). After the correction for initial  $^{230}\text{Th}/^{232}\text{Th}$ , the StalAge algorithm was applied (Scholz and

Hoffmann, 2011). According to obtained age model (Fig. 2a and Supplementary Table S1), C8 grew between  $120.2 \pm 0.7$  kyr BP and  $98.5 \pm 1.0$  kyr BP, covering the end of marine isotope stage (MIS) 5e, the whole of MIS 5d, and the onset of MIS 5c. Three main successive intervals of stalagmite growth can be recognised. The first one, which comprises the lowest 48 cm of the sample, grew between  $\sim 120.2$  and  $\sim 114.0$  kyr BP, and is characterised by an average growth rate of  $\sim 72 \mu\text{m}/\text{yr}$ . The second interval is  $\sim 11$  cm long and was deposited during the  $\sim 114.0$ – $100.3$  kyr BP time span, with an average growth rate of about 1/10 of that of the previous interval. The third interval, recorded in the upper  $\sim 8$  cm of the stalagmite, covers the time interval between  $\sim 100.3$  and  $\sim 98.5$  kyr BP and shows a moderately recovered growth rate ( $\sim 46 \mu\text{m}/\text{year}$ ).

#### 5. Palaeomagnetic results

##### 5.1. Rock magnetic results

IRM acquisition curves indicate major contributions from low coercivity minerals (Fig. 3a), but variable amounts of high coercivity minerals can be also observed, especially in light-brown samples. Only ferrimagnetic minerals are detected in white samples. The low coercivity IRM is thermally demagnetized at 550 °C (Fig. 3b) indicating the presence of magnetite. Maximum unblocking temperatures over 550 °C of the high coercivity component suggest the additional presence of haematite in light-brown samples.

Detailed analysis of ARM and IRM demagnetisation curves has been performed in selected samples (Fig. 3c). These analyses also indicate the presence of two magnetic phases in light-brown samples (Fig. 3d and e) and one magnetic component in white samples. A low coercivity component with a median destructive field (MDF) of 24.1 mT of saturation ARM (SARM) and 20.5 mT of saturation IRM (SIRM) predominates in all samples. The high coercivity component exhibits MDF values  $> 200$  mT (light-brown samples). Detailed thermal demagnetisation of IRM acquired at 300 mT shows a wide distribution of unblocking temperatures up to a maximum of 575 °C. Similar magnetic properties for the low coercivity phase have also been found in British speleothems (Perkins and Maher, 1993). The magnetic

**Table 1**  
 $^{230}\text{Th}$  dating results for stalagmite C8 by ICP-MS analysis.

Sample ID	Distance <sup>a</sup> (mm)	$^{238}\text{U}^b$ (ppb)	$^{232}\text{Th}^b$ (ppt)	$\delta^{234}\text{U}$ measured <sup>c</sup>	$[\text{}^{230}\text{Th}/\text{}^{238}\text{U}]$ activity <sup>d</sup>	Age (kyr, uncorrected)	Age <sup>e,f</sup> (kyr, corrected)	$\delta^{234}\text{U}_{\text{initial}}$ corrected <sup>g</sup>
C8-1	643	149.6 ± 0.5	1385 ± 6	142 ± 4	0.698 ± 0.004	100.2 ± 1.1	99.2 ± 1.2	187 ± 5
C8-3	579	92.3 ± 0.3	2949 ± 11	72 ± 4	0.667 ± 0.005	104.5 ± 1.4	100.6 ± 2.4	96 ± 5
C8-15	534	41.1 ± 0.2	46 ± 3	97 ± 4	0.714 ± 0.005	112.1 ± 1.6	111.9 ± 1.6	133 ± 6
C8-16	485	166.4 ± 0.6	289 ± 4	163 ± 3	0.772 ± 0.005	114.6 ± 1.3	114.4 ± 1.3	225 ± 5
C8-18	393	173.6 ± 0.6	6682 ± 29	91 ± 3	0.737 ± 0.005	119.7 ± 1.7	115.0 ± 2.9	126 ± 5
C8-20	352	151.5 ± 0.7	231 ± 3	107 ± 4	0.734 ± 0.005	115.5 ± 1.5	115.3 ± 1.5	150 ± 6
C8-22	293	184.6 ± 0.6	489 ± 3	96 ± 3	0.730 ± 0.004	116.6 ± 1.4	116.3 ± 1.4	134 ± 5
C8-24	243	123.3 ± 0.5	1187 ± 5	85 ± 4	0.725 ± 0.005	117.6 ± 1.6	116.5 ± 1.6	118 ± 6
C8-27	175	158.1 ± 0.6	418 ± 4	93 ± 4	0.735 ± 0.004	118.7 ± 1.5	118.4 ± 1.5	130 ± 5
C8-28	143	160.2 ± 0.6	1030 ± 6	90 ± 4	0.736 ± 0.005	119.7 ± 1.6	118.9 ± 1.7	126 ± 5
C8-30	83	155.3 ± 0.6	284 ± 4	78 ± 4	0.727 ± 0.005	119.8 ± 1.6	119.6 ± 1.6	109 ± 5
C8-32	36	187.2 ± 0.7	120 ± 4	90 ± 4	0.737 ± 0.004	120.0 ± 1.5	119.9 ± 1.5	126 ± 5

Analytical errors are  $2\sigma$  of the mean.

<sup>a</sup> Distance from base of sample C8, measured along the stalagmite growth axis.

<sup>b</sup> ppb=parts per billion; ppt=parts per trillion.

<sup>c</sup>  $\delta^{234}\text{U} = ((^{234}\text{U}/^{238}\text{U})_{\text{activity}} - 1) \times 1000$ .

<sup>d</sup>  $[\text{}^{230}\text{Th}/\text{}^{238}\text{U}]_{\text{activity}} = 1 - e^{-\lambda_{230}T} + (\delta^{234}\text{U}_{\text{measured}}/1000)(\lambda_{230}/(\lambda_{230} - \lambda_{234}))(1 - e^{-(\lambda_{230} - \lambda_{234})T})$ , where  $T$  is the age. Decay constants are  $9.1788 \times 10^{-6} \text{ yr}^{-1}$  for  $^{230}\text{Th}$ ,  $2.8263 \times 10^{-6} \text{ yr}^{-1}$  for  $^{234}\text{U}$ , and  $1.55125 \times 10^{-10} \text{ yr}^{-1}$  for  $^{238}\text{U}$  (Cheng et al., 2000).

<sup>e</sup> The degree of detrital  $^{230}\text{Th}$  contamination is indicated by the  $[\text{}^{230}\text{Th}/\text{}^{232}\text{Th}]$  atomic ratio instead of the activity ratio.

<sup>f</sup> Age corrections were calculated using an initial  $^{230}\text{Th}/^{232}\text{Th}$  atomic ratio of  $2.0 \times 10^{-5} \pm 1.0 \times 10^{-5}$  to get all dates into stratigraphic order.

<sup>g</sup>  $\delta^{234}\text{U}_{\text{initial}}$  corrected was calculated based on  $^{230}\text{Th}$  age ( $T$ ), i.e.,  $d^{234}\text{U}_{\text{initial}} = d^{234}\text{U}_{\text{measured}} \text{Xe}^{234T}$ , and  $T$  is corrected age.

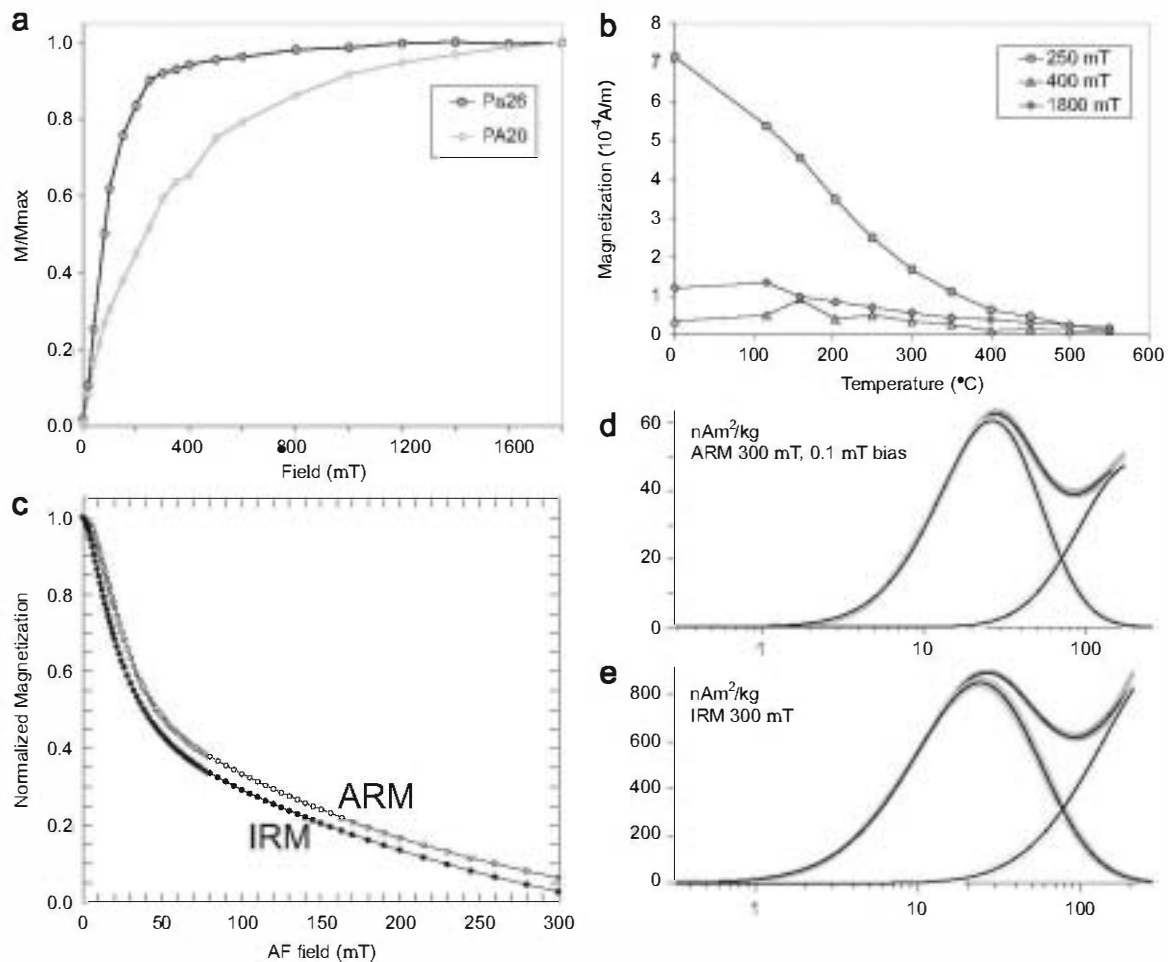


**Fig. 3.** Rock magnetic results. (a) IRM acquisition curve of a white (PA26) and a light-brown (PA20) sample. (b) Thermal demagnetisation curve of three orthogonal IRM components (white sample). (c) Detailed AF demagnetisation of ARM and IRM of a light-brown sample. The maximum applied field was 300 mT. (d, e) Coercivity spectrum of the ARM (d) and IRM (e) components.

properties observed in speleothems seem to be in agreement with pedogenic or extracellular magnetite (Egli and Lowrie, 2003; Egli, 2004, Fig. 4). In summary, rock magnetic studies suggest

the presence of fine-grained magnetite in the stalagmite samples as the main magnetic carrier of NRM and variable contribution of haematite in light-brown samples.

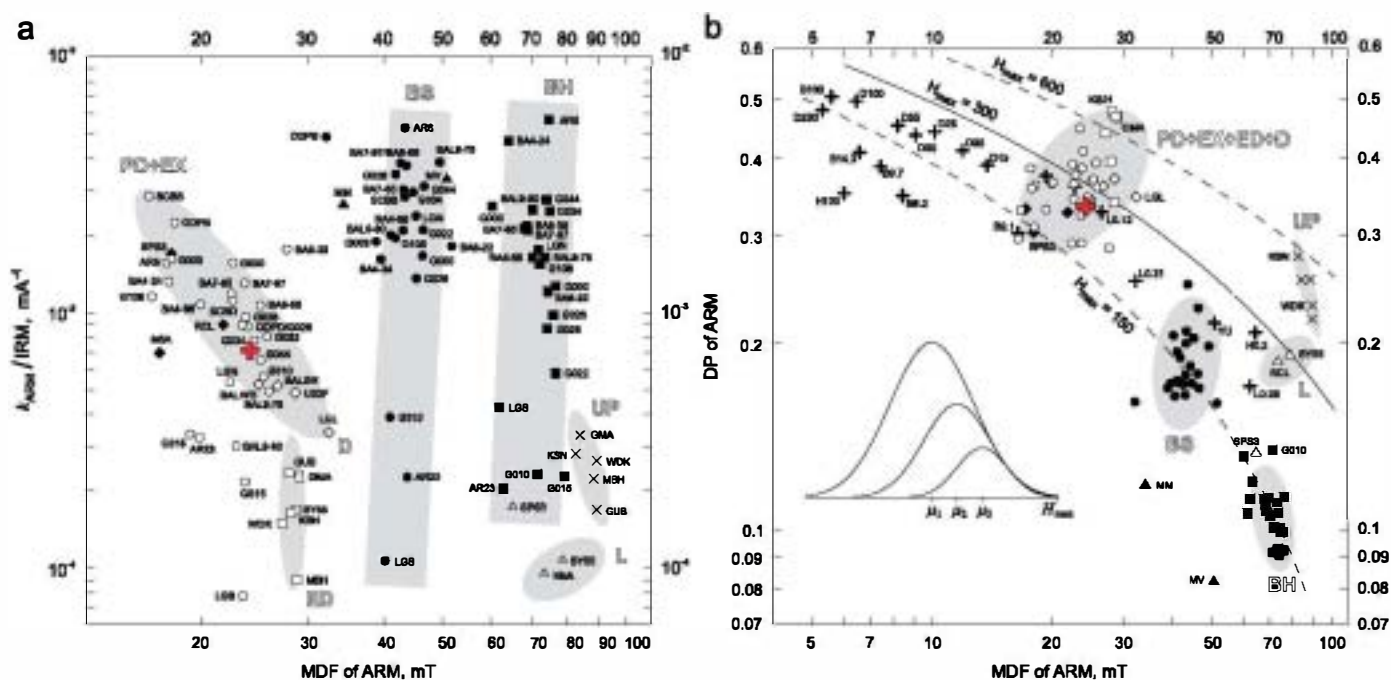


**Fig. 4.** Summary of the ARM and IRM properties for iron spinel components identified by Egli (2004) and results from C8 stalagmite samples. (a) MDF of ARM and kARM/IRM values. Different clusters are indicated by grey ellipses and rectangles, whose extension is equal to four times the standard deviation of the scattered magnetic properties of the components in each cluster. ● outlined letters classify the components: BS (dots): low-coercivity magnetosomes (biogenic soft); BH (squares): high-coercivity magnetosomes (biogenic hard); EX (circles): ultrafine extracellular magnetite; PD (diamonds): pedogenic magnetite; D (open diamonds): detrital particles transported in water systems; ED (open squares): wind-blown particles (aeolian dust); UP (crosses): atmospheric particulate matter produced by urban pollution and L (open triangles): maghemite component in loess. (b) MDF of ARM and DP of ARM values. Data from synthetic magnetites (+ symbols) are reported for comparison. Red (grey) crosses indicate the values measured in a brown sample from the C8 stalagmite. Magnetic properties of stalagmite sample fall into the cluster labelled with PD+EX. (For interpretation of the references to colour in this figure legend, the reader is referred to the web version of this article.)

## 5.2. NRM results

C8 is formed by nearly pure calcite, and as a consequence the magnetic intensity is very low. The initial NRM values ranged between  $0.4$  and  $21.8 \times 10^{-5}$  A/m (Fig. 2c and Supplementary Table S1). The highest NRM intensities were found in samples located in the upper 5 cm of the stalagmite. The lowest values were found in white calcite samples (from  $4.0$  up to  $12 \times 10^{-6}$  A/m). Due to the low NRM intensities, the sample holder was demagnetised before each demagnetisation step and the magnetisation of the sample holder was measured before each measurement and subtracted from the magnetisation of the samples.

All samples exhibited upon demagnetisation a directionally stable low-coercivity/low-unblocking temperature component that is considered as the characteristic remanent magnetisation (ChRM) carried by fine magnetite. In spite of the low intensities of some samples the ChRM could be isolated both during AF (up to 50–80 mT) and thermal demagnetisation (up to 350–500 °C). The ChRM exhibited both, normal and reversed directions (Fig. 5).

Internal consistency has been observed between the magnetic polarity of the ChRM and sample position within the stalagmite (Fig. 2d and e and Supplementary Table S1). All samples from the upper part of the stalagmite have normal polarity. An excursions event is suggested by four samples with largely fluctuating declinations and shallow, partly negative inclinations, located about 50 cm from the base of the stalagmite. Below this interval, two consecutive samples have normal polarities. Three reversed samples were identified in the central part of the stalagmite (~35–40 cm from the base). In addition to these two clear reversed zones, three samples at ~15 cm from the base of the stalagmite exhibit deviating westerly declinations of more than  $45^\circ$ W and very shallow, in one case negative, inclinations. The two directionally anomalous zones, from younger to older, have

been labelled B1 and B2 and the less clear anomalous zone, found at the base of the stalagmite, has been named B3 (Fig. 2f). The excursions events have been defined when the virtual geomagnetic pole (VGP) exhibited a deviation of more than  $40^\circ$  from the geographic pole. The frontiers of polarity intervals were calculated by linear interpolation.

In light-brown samples a higher coercivity-high unblocking temperature component carried by haematite could also be identified. This component always has normal polarity and is not present in samples consisting mostly of white calcite. The mean direction of the second component carried by haematite has a declination  $D=2.6^\circ$  and an inclination  $I=52.6^\circ$  ( $N=14$ ,  $k=12$ ,  $\alpha_{95}=11.9^\circ$ ), close to the present day field direction. It is considered as a secondary component.

## 6. Discussion

### 6.1. Features and age of the Blake event in speleothem C8

For the first time an excursion of the Earth's magnetic field has been recognised in a stalagmite and it has been accurately dated by means of the U–Th disequilibrium technique. Our results support the existence of a geomagnetic polarity excursion characterised by a twofold reversal feature: B1 and B2 (Fig. 2c–f). The B2 event began at about  $116.5 \pm 0.7$  kyr BP. It is well documented and reflects a full reversal of the geomagnetic field that ended at  $114.9 \pm 0.9$  kyr BP. The B1 feature is not so well defined in C8 probably due to a decrease in stalagmite growth rate. The B1 event started at  $114.3 \pm 0.9$  kyr BP (anomalous directions) and ended at  $112.0 \pm 1.9$  kyr BP. We assign these reversals to the Blake geomagnetic polarity event and estimate its duration to be about 4.5 kyr on the basis of our new U–Th age data.  $\delta^{18}O$

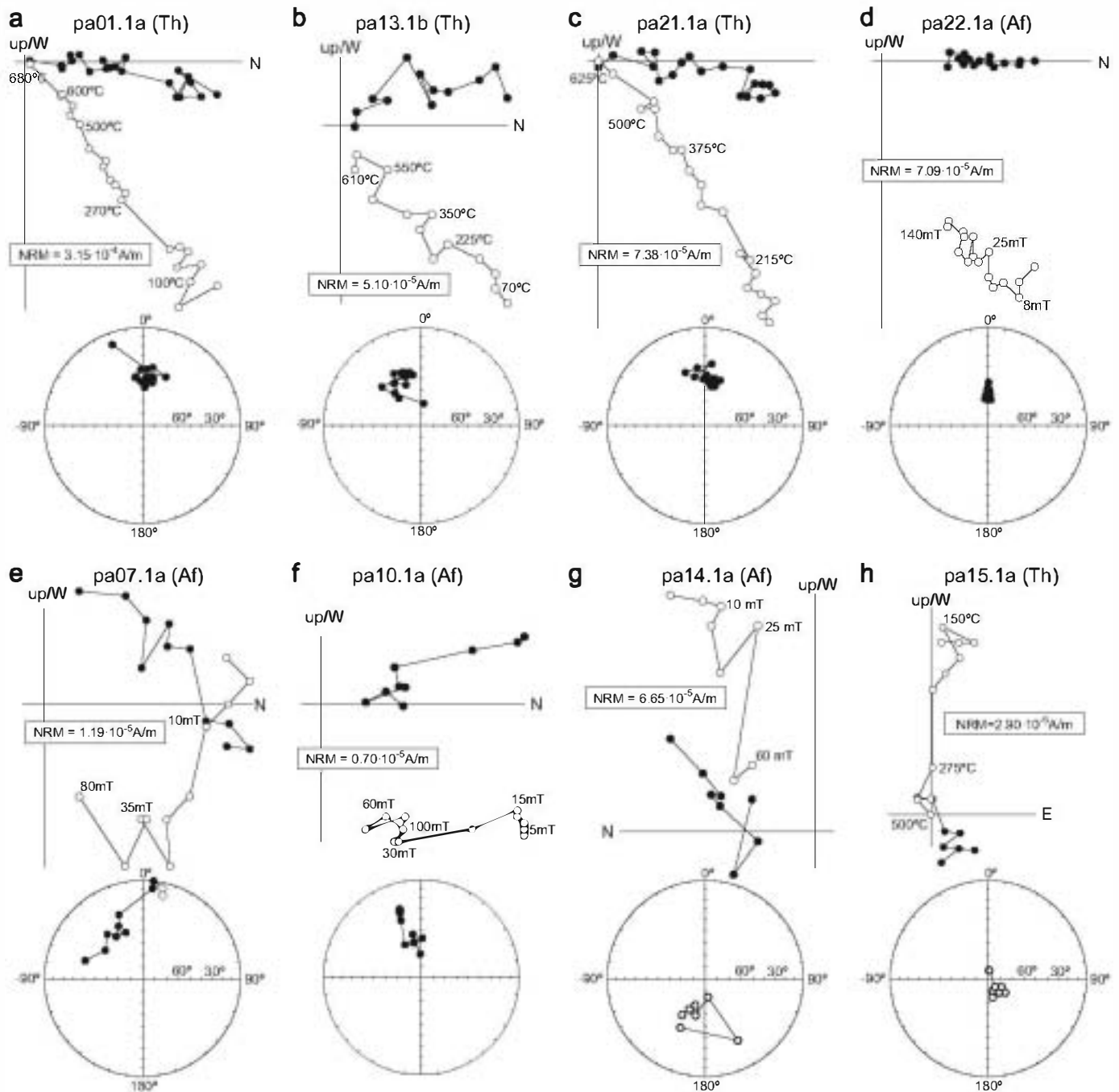


**Fig. 5.** Demagnetisation results of representative samples. ● Orthogonal vector diagrams and stereographic projections during thermal and AF demagnetisation of samples with normal polarity (a, b, c, d), anomalous (e, f) and reversed polarity (g, h). Light-brown samples (a, c, d, e, f) and white samples (b, g, h) are shown. Closed and open symbols: projections onto horizontal and vertical planes, respectively.

analyses performed along the growth axis of the stalagmite locate the excursion in the marine isotope substages 5e/5d, in agreement with marine records of the **Blake** event (Lund et al., 2006; Thouveny et al., 2004). There is also weak evidence for a short angular departure (**B3**) of more than 45° from the dipolar field between  $119.3 \pm 0.8$  and  $118.3 \pm 0.7$  kyr **BP**. No complete reversal is observed at this time.

The age (116.5–112.0 kyr **BP**) and total duration (4.5 kyr) of the polarity changes recorded in the speleothem seem to be consistent with data from Chinese loess obtained by Zhu et al. (1994). Their age estimations for the boundaries of the **Blake** event were  $117.10 \pm 1.2$  up to  $111.8 \pm 1.0$  kyr.

The duration of the event is also consistent with the 5.5 kyr proposal of Fang et al. (1997) obtained from Chinese palaeosols. They place the beginning of the event at an age of 119.97 kyr while we have estimated an age of  $116.5 \pm 0.7$  kyr. We might also consider the **B3** anomaly, defined by a set of three samples with anomalously low inclinations (one negative) found at levels dated from  $119.3 \pm 0.8$  up to  $118.3 \pm 0.7$ , as the beginning of the excursion. It is a short, low angle departure from the dipolar field. But, if **B3** is the first event recorded in the loess palaeosols, then the last reversed episode **B1** would be missing in that record. The estimated duration for the two reversals of Fang et al. (1997) is 1.3 kyr (for the older) and 2.6 kyr (for the younger), which

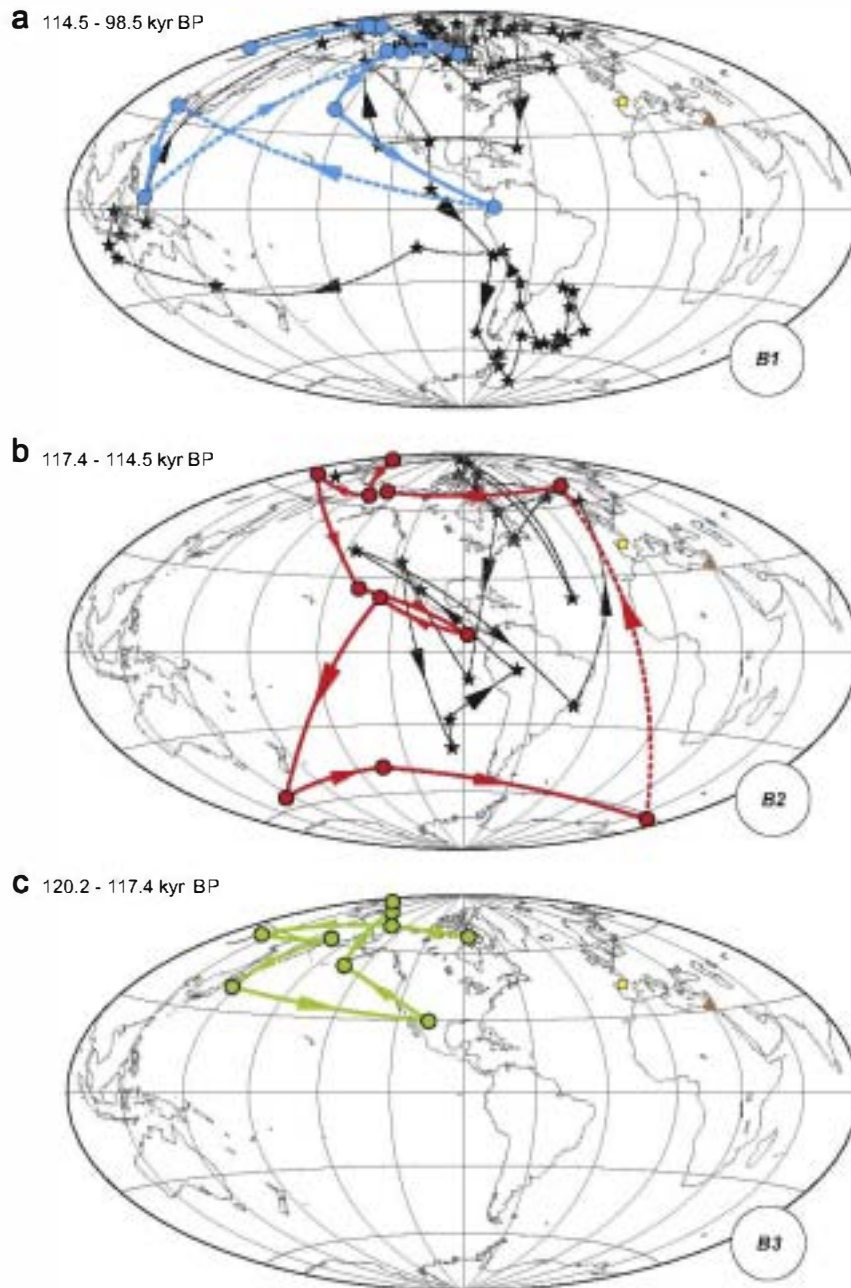


**Fig. 6.** Plots of the VGP path during the Blake event recorded in stalagmite C8. From younger to older: B1 (a) and B2 (b) reversed episodes and (c) the B3 deviator episode. Data of the Blake event according to Tric et al. (1991) are shown in black stars. Location of studied sites: square: Cobre Cave, Northern Spain, this study; triangle: Eastern Mediterranean marine sedimentary core studied by Tric et al. (1991).

seems to be consistent with our observations of 1.6 kyr (B2) and 2.3 kyr (B1), respectively. The discrepancies between the loess-palaeosol record and our stalagmite record could correspond to (a) dating uncertainties associated with the loess-palaeosol profiles, or (b) a lag between the deposition time and the time when the magnetisation was acquired (e.g., Spassov et al., 2003). If magnetisation lock-in was delayed in the loess-palaeosol record, older apparent ages would be expected.

The data scarcity prevents us from defining a detailed VGP path for the transitions in stalagmite C8, but in order to compare our results with previous studies, the VGPs have been plotted in Fig. 6 together with the VGP transitions of the Blake event determined by Tric et al. (1991) (VGP latitude values are also plotted in Fig. 7d and displayed in Supplementary Table S1). Although the differences in resolution are evident, there are some

features in common: (1) the grouping of transitional poles over the East Pacific at low latitudes for the beginning of the B2 episode (Fig. 6b); (2) a southern trajectory close to the American Pacific coast for the beginning of the second event (B1) (Fig. 6a) and (3) the grouping of the poles over SE Asia that defines the end of the Blake event (Fig. 6a).

On the basis of our new U-Th age data, duration of the Blake event is 4.5 kyr, about two times longer than the Laschamp excursion. It also lasts longer than the ~3 kyr timescale predictions proposed by Gubbins (1999). The Blake event, however, is a two-fold well marked reversal in contrast to the single episode Laschamp excursion. It is intriguing that the duration of each reversed episode is within the range observed for single excursions (1.6 kyr for B2 and 2.3 kyr for B1). Laj and Channell (2007) consider that the instability associated to the Blake excursion may

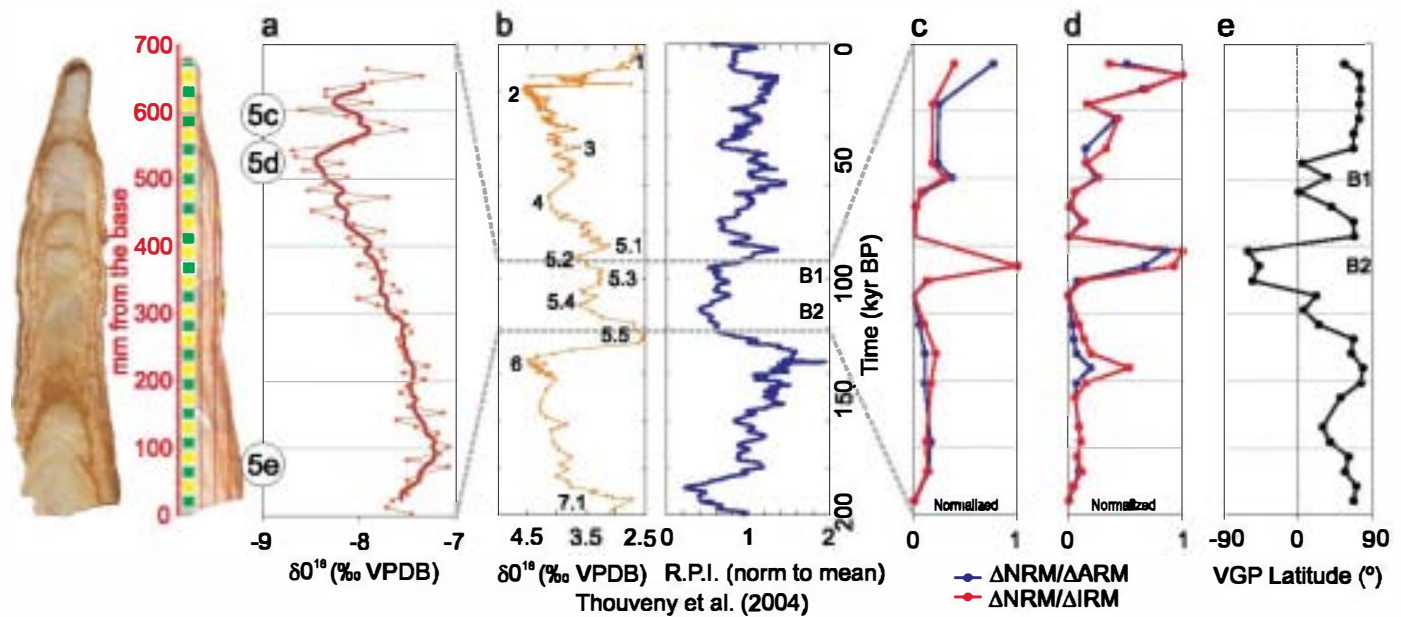


Fig. 7. Relative palaeointensity determinations. Left: studied stalagmite and location of palaeomagnetic samples. (a)  $\delta^{18}\text{O}$  record; (b) isotopic record and RPI values obtained by Thouveny et al. (2004); (c, d) relative palaeointensity determinations of this study (c: in selected samples, d: using all samples) from the low coercivity component in relation to ARM and IRM; (e) VGP latitudes. Dotted grey lines: Proposed correlation.

be explained by the observation that the critical Reynolds number for the onset of core convection is very sensitive to the poloidal field, and the strength of the core convection varies widely in response to changes in magnetic field strength particularly during intensity minima (Zhan and Gubbins, 2000). The origin of excursions remains an open question and accurate determination of their duration can be a key to constrain the geomagnetic models.

## 6.2. Relative palaeointensities

Although C8 is not the ideal candidate to perform relative palaeointensity (RPI) studies (1) because of the presence of two magnetisation components (in some samples), and (2) because the mechanism by which NRM is acquired by speleothems is not yet well understood, we have attempted to construct a relative palaeointensity record by normalising the changes of the NRM (ChRM) by the ARM and IRM contribution of the low coercivity fraction ( $\Delta\text{ARM}$ ,  $\Delta\text{IRM}$ ) (Fig. 7c, Supplementary Table S1). Both normalising parameters yield relative palaeointensity maxima at the time of the B2 reversed (the best recorded) directions and at the normally polarised top of the stalagmite. A more detailed RPI record is presented in Fig. 7d using the  $\Delta\text{NRM}$  for all samples (i.e. including thermally demagnetised samples) relative to the  $\Delta\text{ARM}$  and  $\Delta\text{IRM}$  of close samples of similar lithology. The consistency of the relative RPI highs is clearly documented.

Palaeomagnetic sediment studies have well documented that the Blake excursion occurred within a broad RPI low that extended from around 125 kyr up to 95 kyr (Lund et al., 2006; Thouveny et al., 2004; Valet and Meynadier, 1993). According to our age model, the stalagmite C8 grew mainly within the RPI low providing another possible reason for the low NRM values observed in most of our stalagmite samples. The significance of the RPI maximum located just when the first reversal is completed is remarkable (Fig. 7c–e). Several studies have documented one or two relative maxima within the RPI low (Thouveny et al., 2004, among others), one of which could correspond to the RPI maximum obtained in our study. In addition, high resolution studies of authigenic Be isotopes from NE Atlantic sedimentary sequences indicate that the Blake event is characterised by two maxima in  $^{10}\text{Be}/^9\text{Be}$  concentrations (geomagnetic minima) at 112

and 120 kyr BP (Carcaillet et al., 2004). Our relative maximum is achieved at about 115.0–115.3 kyr, between the two intensity minima. Correlation with RPI records from cores from the Portuguese margin is shown in Fig. 7.

If the RPI data obtained in this study correspond to fluctuations in the intensity of the palaeofield, then the intensity of the geomagnetic field would have increased when the field completely reversed during the B2 event. Under this premise, at least the B2 event could be envisaged as a reversed polarity state with a dipole intensity, partly restored for a short time, which was suddenly aborted in the sense described by Valet et al. (2008).

## 7. Conclusions

A geomagnetic anomaly consisting of two periods of reversed polarity has been documented in a 68 cm-long stalagmite from Cobre Cave, northern Spain. Its characteristic remanent magnetisation is carried by fine-grained magnetite. On the basis of U–Th dates, the anomalous event which is located in the marine substages MIS 5e/5d, occurred during the time interval of the Blake event. The speleothem event is documented by two reversed intervals (B1 and B2), with B2 being clearly reversely magnetised. The age of the event is estimated to be between  $116.5 \pm 0.7$  kyr BP and  $112.0 \pm 1.9$  kyr BP, and has lasted for 4.5 kyr, a slightly longer duration than Laschamp, Mono Lake and Iceland Basin geomagnetic excursions (Laj and Channell, 2007). In addition to these two periods of reversed polarity a low inclination departure (B3) from the dipolar field of more than  $45^\circ$  has also been observed in the time interval  $119.3\text{--}118.3 \pm 0.7$  kyr BP.

Low values of relative palaeointensity during the Blake episode have been recognised which correlates with other sedimentary records of the Blake event. A relative maximum in the palaeofield intensity coeval with the complete reversal during the B2 interval suggests that the B2 interval could be envisaged as a completely reversed polarity state with a dipole contribution partly restored for a short time and then suddenly aborted.

This paper shows the potential of calcite speleothems for the study of geomagnetic excursions. Speleothems can be accurately dated, a crucial point to understand the origin of geomagnetic

excursions. In addition, they do not show important lock-in delays of the magnetisation and present continuous deposition. Their main problems are that calcite speleothems typically have low concentrations of ferromagnetic minerals, thus, generally very weak Natural Remanent Magnetism (NRM) and poor space-resolution. With the recent development of high resolution magnetometers, rapid changes of the geomagnetic field can be reconstructed from speleothems in the near future. Here, for the first time the Blake event has been recognised in a stalagmite from northern Spain for which accurate absolute dating has been carried out using the uranium-series disequilibrium technique.

## Acknowledgements

We greatly thank the permissions given by the Junta de Castilla y León (Spain) for accessing and working in the Fuentes Carrionas-Fuente Cobre Natural Park. The work was carried out with the support of the following Projects/Grants: PR-2007-0111, CGL2007-60618-BTE, CGL2008-02203/BTE, CGL2010-21499-BTE and CGL2011-24790. This paper is a contribution to UCM research groups 910396 “Paleomagnetism” and 910198 “Palaeoclimatology and Global Change”. We thank J.M. Feinberg for the review of a preliminary manuscript.

## Appendix A. Supporting information

Supplementary data associated with this article can be found in the online version at <http://dx.doi.org/10.1016/j.epsl.2012.07.041>.

## References

- Bleil, U., Gard, G., 1989. Chronology and correlation of Quaternary magnetostratigraphy and nanofossil biostratigraphy in Norwegian-Greenland Sea sediments. *Geol. Rundsch.* 78, 1173–1187.
- Carcaillet, J., Bourles, D.L., Thouveny, N., Arnold, M., 2004. An authigenic 10-Be/9-Be record of geomagnetic moment variations and excursions over the last 300 ka. *Earth Planet. Sci. Lett.* 219, 397–412.
- Channell, J.E.T., 2006. Late Brunhes polarity excursions (Mono Lake, Laschamp, Iceland Basin and Pringle Falls) recorded at IODP site 919 (Irminger Basin). *Earth Planet. Sci. Lett.* 244, 378–393.
- Cheng, H., Edwards, R.L., Hoff, J., Gallup, C.D., Richards, D.A., Asmerom, Y., 2000. The half-lives of uranium-234 and thorium-230. *Chem. Geol.* 169, 17–33.
- Creer, K.M., Readman, P.W., Jacobs, A.M., 1980. Palaeomagnetic and palaeontological dating of a section at Gioia Tauro, Italy: identification of the Blake event. *Earth Planet. Sci. Lett.* 50, 289–300.
- Denham, C.R., 1976. Blake polarity episode in two cores from the Greater Antilles outer ridge. *Earth Planet. Sci. Lett.* 29, 422–434.
- Dorale, J.A., Edwards, R.L., Alexander, E.C., Shen, C.-C., Richards, D.A., Cheng, H., 2004. U-series dating of speleothems: techniques, limits, and applications. In: Sasowsky, I.D., Mylroic, J.E. (Eds.), *Studies of Cave Sediments*. Kluwer Academic/Plenum Publishers, New York, pp. 177–197.
- Edwards, R.L., Chen, J.H., Wasserburg, G.J., 1987.  $^{238}\text{U}$ – $^{234}\text{U}$ – $^{230}\text{Th}$ – $^{232}\text{Th}$  systematics and the precise measurement of time over the past 500,000 years. *Earth Planet. Sci. Lett.* 81, 175–192.
- Egli, R., Lowrie, W., 2003. An hysteretic remanent magnetisation of fine magnetic particles. *J. Geophys. Res.* 107 (B10), 2209.
- Egli, R., 2004. Characterization of individual rock magnetic components by analysis of remanence curves, unmixing natural sediments. *Stud. Geophys. Geod.* 48 (2), 391–446.
- Fang, X.M., Li, J.J., Van der Voo, R., Mac Niocaill, C., Dai, X.R., Kemp, R.A., Derbyshire, E., Cao, J.X., Wang, J.M., Wang, G., 1997. A record of the Blake event during the last interglacial paleosol in the western Loess Plateau of China. *Earth Planet. Sci. Lett.* 146, 73–82.
- Frisia, S., Borsato, A., Fairchild, I.J., McDermott, F., 2000. Calcite fabrics, growth mechanisms, and environments of formation in speleothems from the Italian Alps and Southwestern Ireland. *J. Sediment. Res.* 70, 1183–1196.
- Gubbins, D., 1999. The distinction between geomagnetic excursions and reversals. *Geophys. J. Int.* 137, F1–F3.
- Laj, C., Channell, J.E.T., 2007. Geomagnetic excursions. In: *Geomagnetism: Treatise on Geophysics*, vol. 5. Elsevier, pp. 373–416.
- Langereis, C.G., Dekkers, M.J., de Lange, G.J., Paterne, M., van Santvoort, P.J.M., 1997. Magnetostratigraphy and astronomical calibration of the last 1.1 Myr from an eastern Mediterranean piston core and dating of short events in the Brunhes. *Geophys. J. Int.* 129, 75–94.
- Lascu, I., Feinberg, J.M., 2011. Speleothem magnetism. *Quat. Sci. Rev.* 30, 3306–3320.
- Latham, A.G., Schwarcz, H.P., Ford, D.C., Pearce, G.W., 1979a. Palaeomagnetism of stalagmite deposits. *Nature* 280, 383–385.
- Latham, A.G., Schwarcz, H.P., Ford, D.C., Pearce, G.W., 1979b. The paleomagnetism and U–Th dating of three Canadian speleothems: evidence for westward drift, 5.4–2.1 ka BP. *Can. J. Earth Sci.* 19, 1985–1995.
- Latham, A.G., Schwarcz, H.P., Ford, D.C., 1987. Secular variation of the Earth's magnetic field from 18.5 to 15.0 ka BP, as recorded in a Vancouver Island stalagmite. *Can. J. Earth Sci.* 24, 1235–1241.
- Lowrie, W., 1990. Identification of ferromagnetic minerals in a rock by coercivity and unblocking temperature properties. *Geophys. Res. Lett.* 17, 159–162.
- Lund, S., Stoner, J.S., Channell, J.E.T., Acton, G., 2006. A summary of Brunhes palaeomagnetic field variability recorded in Ocean Drilling Programs cores. *Phys. Earth Planet. Inter.* 156, 194–204.
- Muñoz-García, M.B., 2007. Estudio de los espeleotemas recientes de Cueva del Cobre (Palencia) como indicadores de variabilidad paleoclimática. Ph.D. Thesis. Universidad Complutense de Madrid, 307 pp.
- Muñoz-García, M.B., Martín-Chivelet, J., Rossi, C., Ford, D.C., Schwarcz, H.P., 2007. Chronology of Termination II and the Eemian period in Southern Europe based on U–Th dating and stable isotope chronology of stalagmites from Cueva del Cobre (N Spain). *J. Iberian Geol.* 33 (1), 17–30.
- Penshaw, S., Latham, A., Shaw, J., Zhu, X.W., 1993. Preliminary results on recent palaeomagnetic secular variation recorded in speleothems from Xingwen, Sichuan, China. *Cave Sci.* 20 (3), 93–99.
- Perkins, A.M., Maher, B.A., 1993. Rock magnetic and palaeomagnetic studies of British speleothems. *J. Geomagn. Geoelectr.* 45, 143–153.
- Perkins, A.M., 1996. Observations under electron microscopy of magnetic minerals extracted from speleothems. *Earth Planet. Sci. Lett.* 139, 281–289.
- Reinders, J., Hambach, U., 1995. A geomagnetic event recorded in loess deposits of the Tönchesberg (Germany): identification of the Blake magnetic polarity episode. *Geophys. J. Int.* 122, 407–418.
- Roberts, A., 2008. Geomagnetic excursions: knowns and unknowns. *Geophys. Res. Lett.* 35, L17307, <http://dx.doi.org/10.1029/2008GL034719>.
- Rossi, C., Muñoz, A., Cortel, A., 1997. Cave development along the water table in Cobre System (Sierra de Peñalabra, Cantabrian Mountains, N Spain). In: *Proceedings of the 12th International Congress of Speleology, Switzerland*, pp. 179–182.
- Scholz, D., Hoffmann, D., 2011. An algorithm designed for construction of speleothem age models. *Quat. Geochronol.* 6, 369–382.
- Shen, C.C., Edwards, R.L., Cheng, H., Dorale, J.A., Thomas, R.B., Moran, S.B., Weinstein, S., Hirschmann, M., 2002. Uranium and thorium isotopic and concentration measurements by magnetic sector inductively coupled plasma mass spectrometry. *Chem. Geol.* 185, 165–178.
- Shier, M.J., Roebroeks, W., Bakels, C.C., Dekkers, M.J., Brühl, E., De Loecker, D., Gaudzinski-Windheuser, S., Hesse, N., Jagich, A., Kindler, L., Kuijper, W.J., Lurat, T., Mücher, H.J., Penkman, E.H., Richter, D., van Hinsbergen, D.J.J., 2011. Direct terrestrial-marine correlation demonstrates surprisingly late onset of the last interglacial in central Europe 75, 213–218. *Quat. Res.* 75, 213–218.
- Smith, J.D., Foster, J.H., 1969. Geomagnetic reversal in the Brunhes normal polarity epoch. *Science* 163, 565–567.
- Spassov, S., Heller, F., Evans, M.E., Yue, L.P., Dobeneck, T.v., 2003. A lock-in model for the complex Matuyama–Brunhes boundary record of the loess/paleosol sequence at Lingtai (Central Chinese Loess Plateau). *Geophys. J. Int.* 155, 350–366.
- Tauxe, L., 1993. Sedimentary records of relative paleointensity of the geomagnetic field: theory and practice. *Rev. Geophys.* 31, 319–354.
- Thouveny, N., Carcaillet, J., Moreno, E., Leduc, G., Nèrini, D., 2004. Geomagnetic moment variation and palaeomagnetic excursions during the last 400 ka: a stacked record from sedimentary cores of the Portuguese margin. *Earth Planet. Sci. Lett.* 219, 377–396.
- Tric, E., Laj, C., Valet, J.P., Tucholka, P., Guichard, F., 1991. The Blake geomagnetic event: transition geometry, dynamical characteristics and geomagnetic significance. *Earth Planet. Sci. Lett.* 102, 1–13.
- Tucholka, P., Fontugne, M., Guichard, F., Paterne, M., 1987. The Blake magnetic polarity episode in cores from the Mediterranean. *Earth Planet. Sci. Lett.* 86, 320–326.
- Valet, J.P., Meynadier, L., 1993. Geomagnetic field intensity and reversals during the last four million years. *Nature* 366, 235–238.
- Valet, J.P., Plenier, G., Herrero-Bervera, E., 2008. Geomagnetic excursions reflect an aborted polarity state. *Earth Planet. Sci. Lett.* 274, 472–478.
- Zhan, K., Gubbins, D., 2000. Is the geodynamo intrinsically unstable? *Geophys. J. Int.* 140, F1–F4.
- Zhu, R.X., Zhou, L.P., Laj, C., Mazaud, A., Ding, Z.L., 1994. The Blake geomagnetic polarity episode recorded in Chinese loess. *Geophys. Res. Lett.* 21, 697–700.